Role of c-Abl in Directing Metabolic *versus* Mitogenic Effects in Insulin Receptor Signaling*

Francesco Frasca[‡1], Giuseppe Pandini[‡2], Roberta Malaguarnera[‡], Angelo Mandarino[‡], Rosa Linda Messina[‡], Laura Sciacca[‡], Antonino Belfiore[§], and Riccardo Vigneri[‡]

From the [‡]Endocrinologia, Dipartimento di Medicina Interna e di Medicina Specialistica, Università di Catania, Ospedale Garibaldi, Nesima, 95122 Catania and the [§]Endocrinologia, Dipartimento di Medicina Sperimentale e Clinica, Università Magna Graecia, Policlinico Mater Domini, 88100 Catanzaro, Italy

c-Abl is a cytoplasmic tyrosine kinase involved in several signal transduction pathways. Here we report that c-Abl is involved also in insulin receptor signaling. Indeed, c-Abl tyrosine kinase is activated upon insulin stimulation. Inhibition of c-Abl tyrosine kinase by STI571 attenuates the effect of insulin on Akt/GSK-3β phosphorylation and glycogen synthesis, and at the same time, it enhances the effect of insulin on ERK activation, cell proliferation, and migration. This effect of STI571 is specific to c-Abl inhibition, because it does not occur in Abl-null cells and is restored in c-Abl-reconstituted cells. Numerous evidences suggest that focal adhesion kinase (FAK) is involved in mediating this c-Abl effect. First, anti-phosphotyrosine blots indicate that c-Abl tyrosine kinase activation is concomitant with FAK dephosphorylation in response to insulin, whereas c-Abl inhibition is accompanied by FAK phosphorylation in response to insulin, a response similar to that observed with IGF-I. Second, the c-Abl effects on insulin signaling are not observed in cells devoid of FAK (FAK$^{-/-}$ cells). Taken together these results suggest that c-Abl activation by insulin, via a modification of FAK response, may play an important role in directing mitogenic *versus* metabolic insulin receptor signaling.

Insulin and IGF-I receptors (IR and IGF-IR)[3] are heterotetrameric oligomers sharing a high degree of homology. They consist of two extracellular 135-kDa α subunits that contain the ligand domain and two 95-kDa transmembrane β subunits endowed of tyrosine kinase activity (1, 2). Insulin and IGF-I binding to the receptor α subunits stimulates autophosphorylation of the receptor cytoplasmic β tail at multiple tyrosine residues. Activated β subunits interact with and phosphorylate several intracellular substrates at tyrosine residues, including the IRS family proteins (IRS-1/2/3/4) and Gab1 (1, 2). These tyrosine-phosphorylated substrates provide docking sites for SH2-containing proteins, including p85, the regulatory subunits of phosphatidylinositol 3-kinase, and Grb2, a small adapter protein involved in the activation of the Ras pathway (1–3). Activation of the phosphatidylinositol 3-kinase pathway stimulates Akt and, as a consequence, elicits metabolic effects. On the other hand, the recruitment of Grb2 results in the activation of the Ras/ERK pathway, which in turn regulates cell proliferation and differentiation (1–3).

Despite the high similarity between IR and IGF-IR, these two receptors display different effects: IR mainly elicits metabolic effects, including glucose uptake and glycogen synthesis, and IGF-IR mainly stimulates cell proliferation, survival, and differentiation. The mechanisms underlying the different actions of IR and IGF-IR have been extensively studied and are believed to depend on the preferential recruitment and activation of different intracellular substrates, including CrkII, Grb10, 14-3-3, and the focal adhesion kinase (FAK) (1–3).

The FAK is an ubiquitously expressed cytoplasmic tyrosine kinase, involved in integrin and growth factor receptor signaling. It is widely accepted that FAK is a point of convergence in the actions of the extracellular matrix and growth factors (4). FAK tyrosine phosphorylation occurs rapidly in response to growth factor stimulation including PDGF, epidermal growth factor, and IGF-I (4, 5). In particular, FAK phosphorylation at tyrosine 925 creates a binding site for the SH2 domain of Grb2, thereby activating the Ras/ERK pathway (6). Moreover, the activated FAK phosphorylates several adapter proteins including the p130^{CAS} (7) and paxillin (8), which in turn provide docking sites to the small SH2-containing proteins Crk and Nck (7, 9, 10). Similarly to Grb2, also Crk and Nck recruitment results in the activation of the Ras/ERK pathway (4). Because FAK is able to trigger the Ras pathway in response to several stimuli, it has been proposed that FAK plays a major role in mediating the effect of tyrosine kinase receptors on the ERK activation. Evidence supporting this hypothesis was obtained in FAK$^{-/-}$ cells, which exhibit a defect in ERK activation in response to serum and PDGF stimulation (11). Moreover, in NIH3T3 fibroblasts the overexpression of a dominant negative FAK blocks serum-induced activation of ERK (12). At variance with most growth factors, which stimulate FAK phosphorylation, insulin may cause either FAK phosphorylation or dephosphorylation (5, 13,

[1] To whom correspondence should be addressed: Dipartimento di Medicina Interna e di Medicina Specialistica, Endocrinologia, PO Garibaldi Nesima, Via Palermo 636, 95122 Catania, Italy. Tel.: 39-095-759-8827; Fax: 39-095-715-8072; E-mail: f.frasca@unict.it.
[2] Recipient of a fellowship from the American Italian Cancer Foundation.
[3] The abbreviations used are: IR, insulin receptor; IGF, insulin-like growth factor; IGF-IR, IGF-I receptor; ERK, extracellular signal-regulated kinase; FAK, focal adhesion kinase; PDGF, platelet-derived growth factor; FCS, fetal calf serum; PBS, phosphate-buffered saline; MTT, methyl thiazolyl tetrazolium; siRNA, small interfering RNA; GST, glutathione S-transferase.

JOURNAL OF BIOLOGICAL CHEMISTRY **26077**

14), depending on the cell context and experimental conditions, including ligand concentration, cell adhesion, and IR expression level (13, 15–19). This suggests that the inhibition of the integrin/FAK/ERK signaling might play an important role in the metabolic, rather than mitogenic, effect of insulin.

c-Abl, like FAK, is a cytoplasmic tyrosine kinase activated upon cell adhesion (20) and exposure to growth factors like PDGF (21) or hepatocyte growth factor (22). Activated c-Abl tyrosine kinase phosphorylates CrkII, a small SH2/SH3-containing protein involved in cell proliferation and migration (23). Tyrosine 221 phosphorylation by c-Abl results in CrkII inactivation because of intramolecular folding caused by the interaction of the Crk SH2 domain with phosphotyrosine 221 (24). Although the c-Abl role in IR signaling is not known, there is evidence indicating that c-Abl and IR may share common substrates, including the Tub and SORBS1 adapter proteins (25, 26). In particular, Tub is phosphorylated by both IR and c-Abl, whereas SORBS1 may interact with both IR and c-Abl, and this association is insulin-dependent.

Here we show that c-Abl is activated by insulin and regulates the response of FAK to insulin stimulation. Indeed, c-Abl activation leads to FAK dephosphorylation in response to insulin, whereas c-Abl tyrosine kinase inhibition results in FAK phosphorylation in response to insulin. As a consequence, under normal conditions c-Abl activation by insulin promotes Akt/GSK-3β phosphorylation and glycogen synthesis. When c-Abl is inhibited the FAK response to insulin stimulation changes and phosphorylation, cell proliferation and migration are promoted. These data suggest that c-Abl exerts a pivotal role on insulin actions by driving IR signaling to predominant metabolic effects.

EXPERIMENTAL PROCEDURES

Reagents and Compounds—STI571 was by Novartis (Basel, Switzerland). The dimerizer AP20187 was provided by Ariad Pharmaceuticals Inc. (Cambridge, MA). All the other reagents were purchased from Sigma. Anti-Abl monoclonal antibody (Clone 8E9) and anti-FAK polyclonal antibody were purchased from BD PharMingen (San Diego, CA). Anti-Abl (K12) polyclonal antibody and anti-Crk monoclonal antibody were purchased from Santa Cruz Biotechnology Inc. (Santa Cruz, Ca); anti-phosphotyrosine (anti-Tyr(P)) monoclonal antibody 4G10, anti-IRS-1 polyclonal antibody, anti-p85 polyclonal antibody, and anti-Grb2 monoclonal antibody were from Upstate Biotechnology, Inc. (Waltham, MA); anti-phospho p42/44 mitogen-activated protein kinase (Thr[202]/Tyr[204]), anti-mitogen-activated protein kinase, anti-Phospho Akt (Ser[473]), anti-Akt, anti-phospho GSK-3β (Ser[9]), and anti-GSK-3β polyclonal antibodies were from Cell Signaling Technologies (Beverly, MA); and anti-Tyr(P)[925]FAK polyclonal antibody was from BIOSOURCE International (Camarillo, CA). Anti-IR monoclonal antibody (clone MA-20) was provided by Dr. Ira Goldfine (UCSF, San Francisco, CA). Anti-IGF-IR monoclonal antibody (clone αIR-3) was purchased from Oncogene Research (Cambridge, MA). Protein A/G-Sepharose and D-[U-^{14}C]glucose were purchased from Amersham Biosciences (Uppsala, Sweden). IGF-I was purchased from Calbiochem.

Cells—The human hepatoma cell line HepG2 and human breast cancer cell line MCF-7 were purchased from the American Cell Type Culture Collection (Manassas, VA) and cultured in minimum essential medium plus 10% FCS. COS-1 and K562 cells were provided by Dr. Jean Wang (UCSD, La Jolla, CA) and cultured in low glucose Dulbecco's modified Eagle's medium and RPMI plus 10% FCS, respectively. $abl^{-/-}arg^{-/-}$ double knock-out mouse fibroblasts, $abl^{WT}arg^{-/-}$ ($abl^{-/-}arg^{-/-}$ cells infected with MSCV-WTAbl), $abl^{KD}arg^{-/-}$ ($abl^{-/-}arg^{-/-}$ cells infected with MSCV-Abl-kinase defective), and $abl^{+/+}arg^{+/+}$ cells (control fibroblasts from littermate mice) were also provided by Dr. Jean Wang (UCSD, La Jolla, CA) and cultured in high glucose Dulbecco's modified Eagle's medium plus 10% FCS. FAK$^{-/-}$ and FAK$^{+/+}$ (clone R6) mouse fibroblasts were kindly provided by Dr. David Schlaepfer (The Scripps Institute, La Jolla, CA) and were maintained on gelatin-coated (0.1% in phosphate-buffered saline (PBS)) cell culture dishes in Dulbecco's modified Eagle's medium supplemented with 10% FCS, nonessential amino acids for minimal essential medium, sodium pyruvate (1 mM), penicillin (50 units/ml), streptomycin (50 mg/ml), ciprofloxacin (0.02 mg/ml), and G418 (0.5 mg/ml).

Plasmids and Transfections—AblFKBP-WT and AblFKBP-KD plasmids were kindly provided by Dr. Richard Van Etten (Harvard Medical School, Harvard, MA) (27). These constructs contain the FKBP domain, which allows Abl dimerization and activation in the presence of the dimerizer AP20187. All transfections were performed in 6-well plates with FuGENE 6 (Roche Applied Science) according to the manufacturer's instructions (DNA:FuGENE ratio 1:3). The cells were processed 24 h after transfection.

Viability Assay—Cell viability was measured by the methyl thiazolyl tetrazolium (MTT) test (Amersham Biosciences). 10^3 cells were seeded in 96-well plates. After 24 h, complete medium was replaced with serum-free medium containing 0.1% bovine serum albumin. The cells were then incubated with 10 nM of either insulin or IGF-I, in the presence or the absence of 1.0 μM STI571, for additional 48 h. The cells were then incubated with complete medium containing 0.5 mg/ml MTT at 37 °C plus 5% CO_2. 4 h later cells were dissolved in 100 μl of a solution containing dimethyl sulfoxide plus 2.5% complete medium, and formazan absorbance was then read at 405 nm.

Silencing of c-Abl Expression by siRNA—The cells were plated onto six-well plates (10^5/well), maintained in antibiotic-free medium for 24 h, and transfected with a mixture containing Opti-MEM, 8 μl/well Lipofectamine 2000 (Invitrogen, San Diego, CA), and either 0.5 μg/well scramble small interfering RNA (siRNA) or a mixture of four c-Abl siRNA (Dharmacon Research, Inc., Lafayette, CO) for 5 h. The sequences of these siRNAs are available from the manufacturer, and their specificity has been tested by microarray analysis. The cells were then incubated with fresh medium for 48 h, serum-starved for 24 h and incubated with or without 1.0 μM STI571 in serum-free medium for 2 h. Then 10 nM of either insulin or IGF-I were added for 5 min, or longer, as indicated in the different experiments.
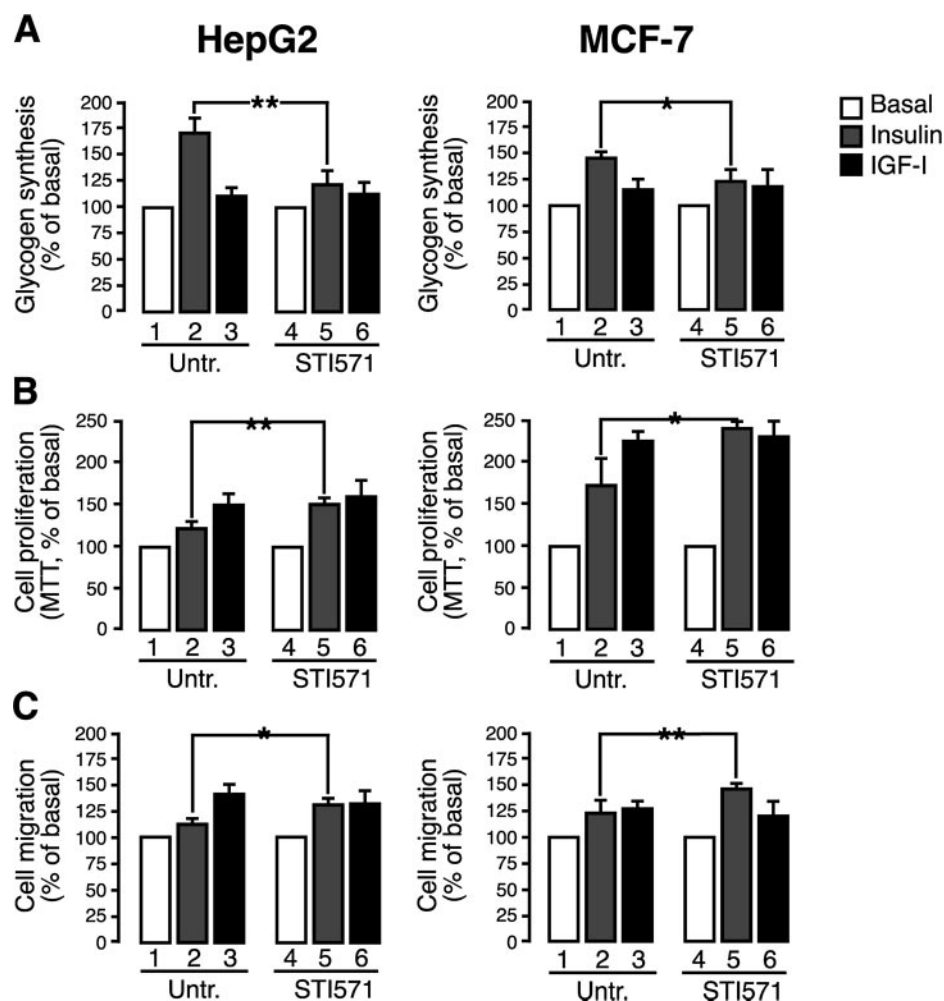
A

B

C

FIGURE 1. **Effect of c-Abl inhibition by STI571 on cell response to insulin and IGF-I.** *A*, glycogen synthesis. HepG2 (*left panel*) and MCF-7 (*right panel*) cells were serum-starved and incubated in the absence (*bars 1–3*) or the presence (*bars 4–6*) of 1 μM STI571 in low glucose medium as described under "Experimental Procedures." Glycogen synthesis in the absence (*white bars*) or the presence of 10 nM insulin (*gray bars*) or IGF-I (*black bars*) was evaluated as [^{14}C]glucose incorporation into glycogen. The numbers are expressed as percentages of basal and are the means ± S.D. of three separate experiments performed in triplicate. **, $p < 0.01$. *B*, cell proliferation. HepG2 and MCF-7 cells were plated onto 96-multiwell and grown for 5 days in the absence (*bars 1–3*) or the presence (*bars 4–6*) of 1 μM STI571 and the indicated growth factors. *White bars*, unstimulated cells; *gray bars*, cells stimulated with 10 nM insulin; *black bars*, cells stimulated with 10 nM IGF-I. After incubation with MTT, the plates were read at 590 nm as described under "Experimental Procedures." The values are expressed as percentages of basal and are the means ± S.D. of three separate experiments performed in triplicate. **, $p < 0.01$. *C*, cell migration. HepG2 and MCF-7 cells were first incubated in the absence (*bars 1–3*) or the presence (*bars 4–6*) of 1 μM STI571 as described under "Experimental Procedures." The cells were then collected and allowed to migrate in the lower side collagen-coated transwells for 6 h in the absence (*white bars*) or presence of either 10 nM insulin (*gray bars*) or IGF-I (*black bars*) in the presence (*bars 4–6*) or the absence (*bars 1–3*) of 1 μM STI571. The values are expressed as percentages of basal and are the means ± S.D. of three separate experiments performed in triplicate. *, $p < 0.05$. *Untr.*, untreated.

Migration Assay—Migration assay was performed as previously described (38) with some modifications. Subconfluent cells were preincubated with or without 1.0 μM STI571 for 1 h. Following preincubation, the cells were then detached with Trypsin-EDTA, collected, and resuspended at 10^6/ml. 10^5 cells, in serum-free medium (100 μl), were placed on 6.5-mm-diameter polycarbonate filters (8-μm pore size; Costar) and coated at the lower side with 250 μg/ml collagen IV. Then filters were placed over bottom chambers containing 500 μl of serum-free medium with or without 10 nM of ligand (either insulin or IGF-I) and 1.0 μM STI571 and incubated for 6 h at 37 °C with 5% CO_2. At the end of 6 h, the cells on the upper surface of the

filters were removed with a cotton swab, and the filters were stained with crystal violet solution (0.05% crystal violet in PBS + 20% ethanol). The filters were then placed in 24-multiwell plates containing 250 μl/well of 10% acetic acid and incubated for 30 min at room temperature under agitation to elute the dye. The samples were then measured at 590 nm. The row numbers obtained were reported as percentages of basal.

Glycogen Synthesis—The rate of glycogen synthesis was estimated by labeled glucose incorporation into cellular glycogen. The cells were seeded onto 24-multiwell plates. 24 h later complete medium was replaced with serum-free/low glucose medium, and the cells were preincubated with or without 1.0 μM STI571 for 2 h and exposed to 10 nM of either insulin or IGF-I for 30 min at 37 °C. D-[U-^{14}C]Glucose (1.25 μCi/well) was then added for 60 min, and the incorporation was stopped by rapidly washing cells three times with ice-cold PBS. The cells were then solubilized in 30% KOH and transferred to separate tubes, and 2 mg of glycogen was added. Glycogen was then precipitated by adding 2.2 volumes of 100% ethanol, and the radioactivity incorporated into glycogen was measured in a Beckman L6000TA β-counter. The data were normalized for protein content.

Preparation of Cell Lysate and Western Blot—Subconfluent cells were serum-starved for 24 h and incubated with or without 1.0 μM STI571 in serum-free medium for 2 h. Then 10 nM of either insulin or IGF-I were added for 5 min, or longer, as indicated in the different experiments. The cells were washed twice with ice-cold PBS, pH 7.4, and lysed in radioimmune precipitation assay buffer (150 mM NaCl, 1% Nonidet P-40, 50 mM Tris, pH 7.4, 10 mM sodium pyrophosphate, 100 mM NaF, 2 mM phenylmethylsulfonyl fluoride, 2 mM sodium vanadate, 10 μg/ml pepstatin, 10 μg/ml aprotinin, 10 μg/ml leupeptin). After being scraped, the samples were rotated for 15 min at 4 °C. Insoluble material was separated from soluble extract by microcentrifugation at $10,000 \times g$ for 10 min at 4 °C. The protein concentration was determined by the Bradford assay (Bio-Rad). For immunoprecipitation 0.5–1-mg proteins were incubated with 2 μg of the indicated antibodies and pro-
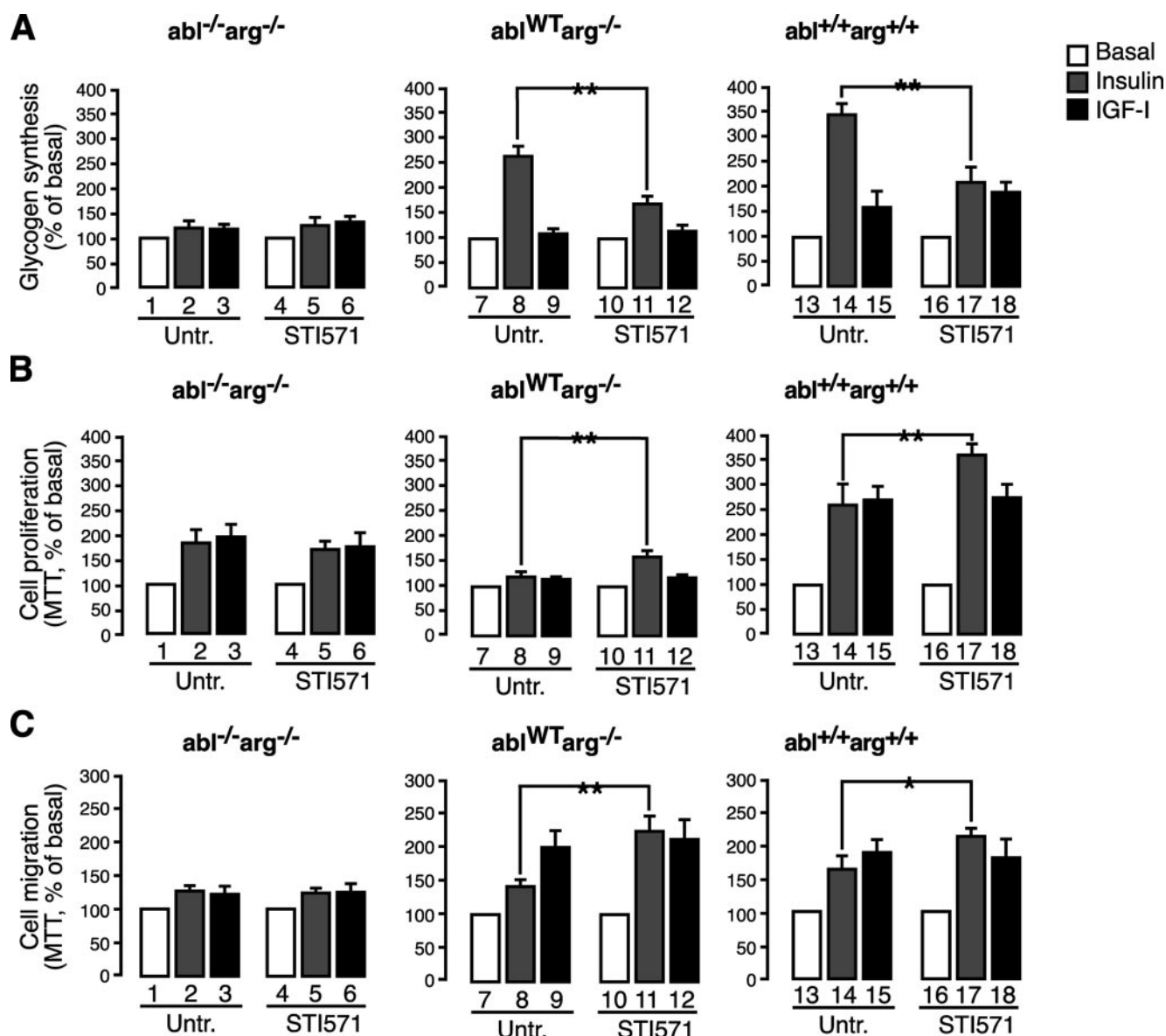
FIGURE 2. **Effect of c-Abl on insulin and IGF-I biological effects: experiments in Abl$^{-/-}$arg$^{-/-}$, abl^{WT}arg$^{-/-}$, and abl$^{+/+}$arg$^{+/+}$ cells.** *A*, glycogen synthesis. The indicated cells were serum-starved and incubated in the absence (*bars 1–3, 7–9,* and *13–15*) or the presence (*bars 4–6, 10–12,* and *16–18*) of 1 μM STI571 in low glucose medium as described under "Experimental Procedures." Glycogen synthesis in the absence (*white bars*) or the presence of 10 nM of either insulin (*gray bars*) or IGF-I (*black bars*) was evaluated as [^{14}C]glucose incorporation into glycogen. The numbers are expressed as percentages of basal and indicate the means ± S.D. of three experiments performed in triplicate. **, $p < 0.01$. *B*, cell proliferation. The cells were plated onto 96-multiwell plates and grown for 5 days in the absence (*bars 1–3, 7–9,* and *13–15*) or the presence (*bars 4–6, 10–12,* and *16–18*) of 1 μM STI571 and the indicated growth factors. *White bars*, unstimulated cells; *gray bars*, cells stimulated with 10 nM insulin; *black bars*, cells stimulated with 10 nM IGF-I. After incubation with MTT, the plates were read at 590 nm as described under "Experimental Procedures." The numbers are expressed as percentages of basal and indicate the means ± S.D. of three separate experiments performed in triplicate. *, $p < 0.05$; **, $p < 0.01$. *C*, cell migration. The cells were first incubated in the absence (*bars 1–3, 7–9,* and *13–15*) or the presence (*bars 4–6, 10–12,* and *16–18*) of 1 μM STI571 as described under "Experimental Procedures." The cells were then collected and allowed to migrate in lower side collagen-coated transwells for 6 h in the absence (*white bars*) or the presence of 10 nM of either insulin (*gray bars*) or IGF-I (*black bars*) in the presence (*gray bars*) or absence (*black bars*) of 1 μM STI571. The numbers are expressed as percentages of basal and indicate the means ± S.D. of three separate experiments performed in triplicate. **, $p < 0.01$. *Untr.*, untreated.

tein A/G-Sepharose. For Western blot on crude cell lysate, after the addition of 5× sample buffer, samples (50 μg of protein) were heated at 95 °C for 10 min. Immunoblotting was performed using 1 μg/ml of the indicated antibodies. All of the immunoblots were revealed by enhanced chemiluminescence (Amersham Biosciences), autoradiographed, and subjected to densitometric analysis. The densitometric results were corrected for the total protein content.

c-Abl in Vitro Kinase—The cells were incubated as above and lysed with radioimmune precipitation assay buffer. After protein

content normalization, immunoprecipitation was performed with anti-c-Abl polyclonal antibody (K12). The beads were then incubated for 40 min with 20 μl of a kinase mixture containing 1 μg of GST-Crk (kindly provided by Prof. Hidesaburo Hanafusa, Japan), 10 μM ATP, in 10 mM Tris, pH 7.4, 10 mM MgCl$_2$, 1 mM dithiothreitol. The reaction was then stopped with Laemmli buffer, and the samples were boiled for 10 min. After SDS-PAGE, filters containing c-Abl and phosphorylated Crk were probed with 4G10 monoclonal antibody and reprobed with either monoclonal anti-c-Abl (8E9) or polyclonal anti-Crk antibody (Santa Cruz).
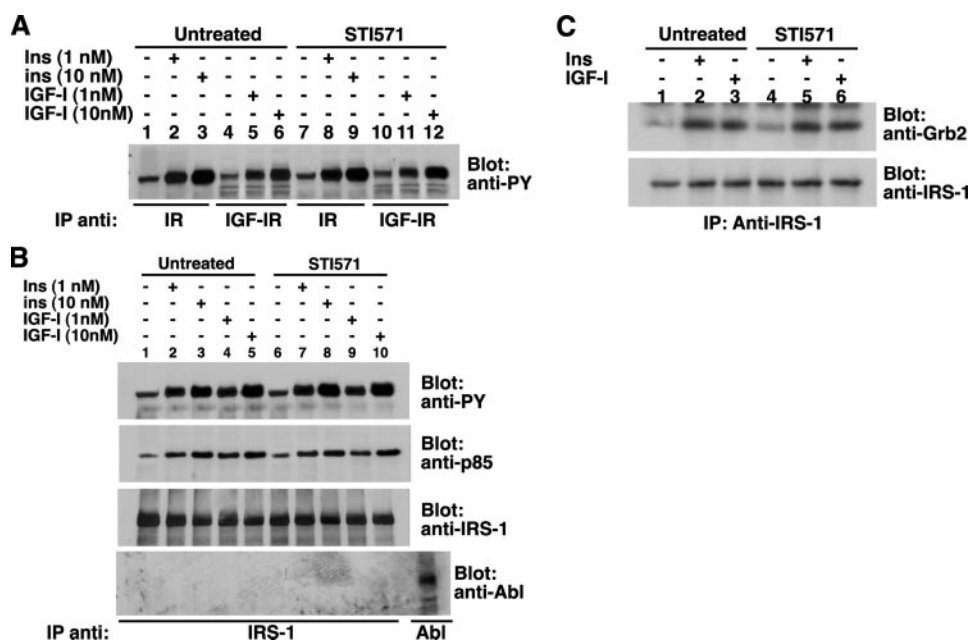
FIGURE 3. Effect of STI571 on proximal events in IR and IGF-IR signaling in HepG2 cells. The cells were serum-starved and incubated in the presence or absence of 1 μM STI571 as described under "Experimental Procedures." *A*, anti-phosphotyrosine Western blots of IR and IGF-IR immunoprecipitated (*IP*) from cells incubated in the absence (*lanes 1*, *4*, *7*, and *10*) or the presence of either insulin (1 or 10 nM, *lanes 2* and *8* and *lanes 3* and *9*, respectively) or IGF-I (1 or 10 nM, *lanes 5* and *11* and *lanes 6* and *12*, respectively). *B*, Western blots of anti-IRS-1 immunoprecipitates. *Lanes 1* and *6*, unstimulated cells; *lanes 2* and *7*, cells treated with 1 nM insulin; *lanes 3* and *8*, cells treated with 10 nM insulin; *lanes 4* and *9*, cells treated with 1 nM IGF-I; *lanes 5* and *10*, cells treated with 10 nM IGF-I. The blots were performed with antiphosphotyrosine antibody (*upper panel*), anti-p85 antibody (*middle upper panel*), anti-IRS-1 antibody (*middle lower panel*), and probing with anti-Abl antibody (*lower panel*). *C*, anti-Grb2 Western blotting on anti-IRS-1 immunoprecipitates (*upper panel*) and reprobing with anti-IRS-1 antibody (*lower panel*) in cells unstimulated (*lanes 1* and *4*) or treated with 10 nM of either insulin (*lanes 2* and *5*) or IGF-I (*lanes 3* and *6*). The pictures shown are representative of three separate experiments.

Statistical Analysis—Densitometry results were obtained by using ImageJ 1.37 software (National Institutes of Health). Densitometry results obtained with phosphorylated proteins were normalized for total protein content. The numbers were then expressed as percentages of basal. Cell viability, migration, and glycogen synthesis and densitometry results in response to either insulin or IGF-I, with or without STI571 were compared by two-way analysis of variance. Statistical analysis was carried out with Microsoft Excel software.

RESULTS

Insulin Biological Effects Are Influenced by the Inhibition of c-Abl Tyrosine Kinase Activity—To explore whether c-Abl tyrosine kinase is involved in insulin biological effects, we incubated HepG2 (Fig. 1, *left panel*) and MCF-7 cells (Fig. 1, *right panel*) in the presence or the absence of the Abl inhibitor STI571 and evaluated both metabolic (glycogen synthesis) and nonmetabolic effects (cell proliferation and migration) in response to insulin. In these experiments insulin effects were compared with the effects induced by IGF-I (Fig. 1). c-Abl inhibition by 1 μM STI571 decreased the glycogen synthesis in response to insulin (Fig. 1*A* compare *bar 2* with *bar 5*). In contrast, evaluation of cell proliferation by MTT assay indicated that exposure to STI571 significantly enhanced the effect of insulin on cell proliferation (Fig. 1*B*, compare *bar 2* with *bar 5*) and migration (Fig. 1*C*, compare *bar 2* with *bar 5*). STI571 effect was not observed on IGF-I stimulation (Fig. 1, compare *bars 3* with *bars 6*) and was similar in both cell types.

In these experiments STI571 changed cell responses to insulin and abrogated the differences existing between insulin and IGF-I stimulation (Fig. 1, *A* and *B*, compare *bars 2* and *3* with *5* and *6*). These data suggest that c-Abl activation may contribute to differentiate IR from IGF-IR signaling by selectively increasing the metabolic effects and decreasing the nonmetabolic effects of the IR signaling pathway.

A Functional c-Abl Kinase Influences IR Biological Effects—To assess by a different procedure whether the effect of STI571 on insulin actions is specifically mediated by c-Abl tyrosine kinase inhibition, fibroblasts derived from *abl* and *arg* double knock-out mice ($abl^{-/-}arg^{-/-}$ cells) were also used (28). These cells are devoid of both c-Abl and the related kinase Arg (*abl* related gene), a cytoplasmic tyrosine kinase with overlapping functions with c-Abl, which is also a target of STI571. As a control, $abl^{-/-}arg^{-/-}$ cells reconstituted with murine c-Abl by retroviral gene transfer ($abl^{WT}arg^{-/-}$ cells) were also used.

STI571 did not affect glycogen synthesis in response to insulin in $abl^{-/-}arg^{-/-}$ cells (Fig. 2*A*, compare *bar 2* with *bar 5*), whereas it inhibited glycogen synthesis in response to insulin in $abl^{WT}arg^{-/-}$ cells (Fig. 2*A*, compare *bar 8* with *bar 11*) in a manner similar to that observed in HepG2 cells (Fig. 1*A*). In $abl^{-/-}arg^{-/-}$ cells, STI571 did not enhance the effect of insulin on cell proliferation and migration (Fig. 2, *B* and *C*, compare *bars 2* with *bar 5*). In contrast, STI571 enhanced cell proliferation and migration in response to insulin in $abl^{WT}arg^{-/-}$ cells (Fig. 2, *B* and *C*, compare *bars 8* with *bars 11*) in a manner similar to that observed in HepG2 (Fig. 1*B*). Similar results were observed with $abl^{+/+}arg^{+/+}$ cells, which are control fibroblasts derived from littermates (Fig. 2, compare *bars 14* with *bars 17*). Moreover, STI571 did not influence insulin effects in $abl^{-/-}arg^{-/-}$ cells retrovirally infected with a kinase defective c-Abl construct ($abl^{KD}arg^{-/-}$, not shown). These data confirm that the effect of STI571 on insulin biological activities is specifically based upon the presence of a functional c-Abl tyrosine kinase and is not dependent on the STI571 influence or other tyrosine kinases. Cell responses to IGF-I were not affected by STI571 (Fig. 2, compare *bars 3–6* and *9* with *bar 12*).

c-Abl Changes the Effect of Insulin on Akt, GSK-3β, and ERK Activation—To explain the mechanisms underlying the effect of c-Abl on insulin actions, intracellular signaling molecules downstream IR were studied by Western blot with anti-phosphotyrosine and phosphospecific antibodies (Figs. 3 and 4).
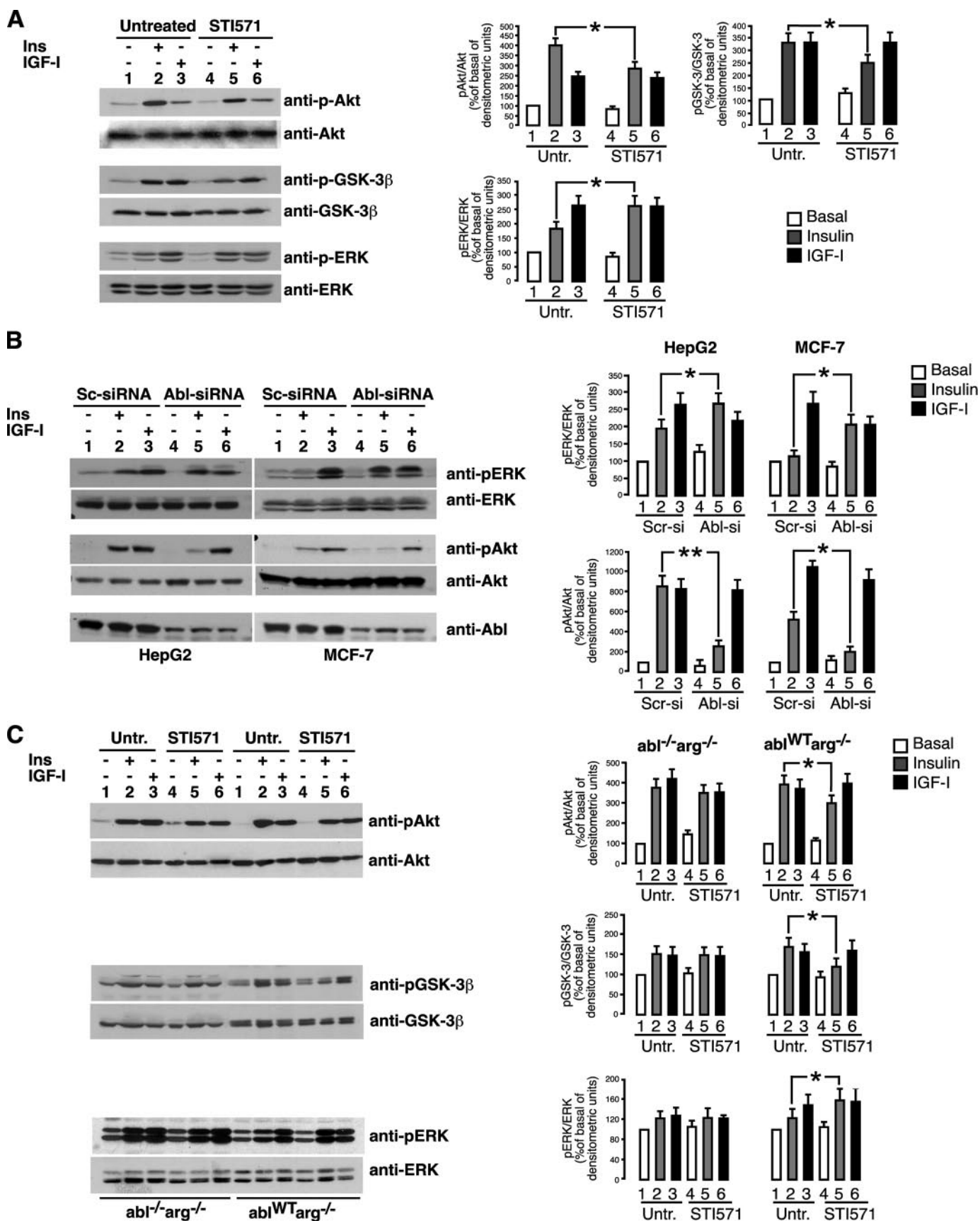
To explore whether STI571 may interfere with IR and IGF-IR proximal signaling events, HepG2 cells were incubated or not with the Abl inhibitor STI571 and signaling pathway activation evaluated by Western blot (Fig. 3). STI571 did not affect IR and IGF-IR autophosphorylation in response to their ligands (insulin: Fig. 3*A*, compare *lanes 2* and *3* with *lanes 8* and *9*; IGF-I: Fig. 3*A*, compare *lanes 5* and *6* with *lanes 11* and *12*). In addition, STI571 did not influence IRS-1 phosphorylation in response to either insulin (Fig. 3*B*, compare *lanes 2* and *3* with *lanes 7* and *8*) or IGF-I (Fig. 3*B*, compare *lanes 4* and *5* with *lanes 9* and *10*), and as a consequence, it did not affect the recruitment of p85 (Fig. 3*B*, compare *lanes 2–5* with *lanes 7–10*) or Grb2 (Fig. 3*C*, compare *lanes 2* and *3* with *lanes 5* and *6*). Moreover, reblotting with anti-c-Abl 8E9 antibody did not detect c-Abl in anti-IRS-1 immunoprecipitates (Fig. 3*B*, *bottom panel*).

In contrast, STI571 significantly attenuated Akt and GSK-3β phosphorylation in response to insulin, whereas it enhanced ERK response (Fig. 4*A*, compare *lane 2* with *lane 5*, ~2-fold increase by densitometric analysis). The responses to IGF-I remained unchanged (Fig. 4*A*, compare *lane 3* with *lane 6*). Because STI571 may inhibit not only c-Abl tyrosine kinase but also other tyrosine kinases such as PDGF-R and c-Kit, we used also additional, specific, and independent mechanisms to inhibit c-Abl and evaluate the consequences on the phosphorylation of downstream mediators. HepG2 and MCF-7 cells were subjected to Abl silencing by siRNA (Fig. 4*B*), and Western blot experiments confirmed that in both HepG2 and MCF-7 cells Abl inhibition reduced Akt and GSK-3β phosphorylation in response to insulin, whereas it enhanced ERK activation (Fig. 4*B*, compare *lanes 2* with *lane 5*). In accordance with the results shown in Fig. 4*A*, the responses to IGF-I remained unchanged (Fig. 4*B*, compare *lane 3* with *lane 6*). Experiments performed in $abl^{-/-}arg^{-/-}$ and $abl^{\mathrm{WT}}arg^{-/-}$ confirmed these results (Fig. 4*C*, compare *lane 2* with *lane 5* and *lane 3* with *lane 6*). Taken together, these data indicate that c-Abl tyrosine kinase inhibition results in reduced Akt/GSK-3β phosphorylation by insulin and enhanced ERK activation, whereas no effect is observed on IGF-I activation.

Insulin Stimulates c-Abl Tyrosine Kinase Activity—We then explored whether c-Abl tyrosine kinase activity is affected by insulin stimulation (Fig. 5). HepG2 cells were stimulated with insulin for the indicated times, and the c-Abl tyrosine kinase activity was evaluated in Abl immunoprecipitates by an *in vitro* kinase assay, using GST-CrkII as a substrate (see "Experimental Procedure"). Anti-Tyr(P) Western blot shown in Fig. 5*A* indicated that after 2 min of insulin stimulation, an increased Crk

phosphorylation by c-Abl is observed and declines within 30–60 min (Fig. 5*A*). Exposure of HepG2 cells for 60 min to 1 μM of the Abl inhibitor STI571 completely abolished Crk phosphorylation, indicating that the tyrosine kinase activity observed in those immunoprecipitates is Abl-specific. In those experiments K562 cells, expressing the constitutively active BCR-Abl oncoprotein, were used as a positive control (Fig. 5*A*, *left panel*). Interestingly, no increase in c-Abl tyrosine kinase activity was observed in HepG2 cells after stimulation with IGF-I (Fig. 5*A*, *right panel*).

We then studied CrkII phosphorylation by c-Abl in living cells (Fig. 5*B*). Although CrkII is a substrate of IGF-IR but not of IR tyrosine kinase (29, 30), insulin is able to stimulate CrkII tyrosine phosphorylation in living cells maybe for the intervention of an unknown kinase (31). We therefore studied CrkII phosphorylation in response to either insulin or IGF-I in HepG2 cells in the presence or the absence of the c-Abl inhibitor STI571 (Fig. 2*B*). Anti-Tyr(P) Western blot performed on anti-CrkII immunoprecipitates revealed that STI571 abolished insulin-induced CrkII phosphorylation *in vivo*, whereas it was without effect on IGF-I-dependent CRKII stimulation (Fig. 5*B*). To confirm the role of c-Abl in mediating CrkII phosphorylation in response to insulin *in vivo*, HepG2 cells were subjected to c-Abl silencing by siRNA (Fig. 5*C*). In accordance with data obtained with STI571, preincubation of HepG2 cells with Abl-siRNA resulted in the abrogation of CrKII phosphorylation in response to insulin (Fig. 5*C*), whereas the response to IGF-I was not affected (Fig. 5*C*). These results suggest that insulin, but not IGF-I, activates c-Abl, which in turn activates CrKII.

c-Abl Changes FAK Response to Insulin Stimulation—On the basis of the results obtained in cells subjected to c-Abl inhibition/silencing, we hypothesized that c-Abl could affect IR signaling and biological effects, making them more similar to those of IGF-IR signaling. A divergent point between IR and IGF-IR signaling is the FAK, whose phosphorylation level may be differently regulated by insulin and IGF-I and may be influenced by Crk activation (13, 14). We therefore evaluated FAK activation in response to either insulin or IGF-I stimulation in HepG2 cells incubated in the presence or the absence of STI571 (Fig. 6*A*). Anti-phosphotyrosine Western blot performed in HepG2 cells showed that insulin induced FAK dephosphorylation (Fig. 6*A*, compare *lane 1* with *lane 2*), whereas IGF-I caused FAK phosphorylation as previously reported (13). However, in the presence of the c-Abl inhibitor STI571, insulin stimulated a relevant FAK phosphorylation (Fig. 6*A*, compare *lane 4* with *lane 5*). To confirm the role of c-Abl tyrosine kinase in mediat-

FIGURE 4. **Effect of c-Abl on downstream mediators of insulin and IGF-I signaling.** *A*, HepG2 were serum-starved and incubated in the presence or absence of 1 μM STI571 as described under "Experimental Procedures." Shown are blots with the indicated anti-phosphospecific antibody on crude lysates from unstimulated cells (*lanes 1* and *4*) or from cells treated with 10 nM of either insulin (*lanes 2* and *5*) or IGF-I (*lanes 3* and *6*). The means ± S.D. of densitometric analyses of three separate experiments are reported on the *right*. *, $p < 0.05$; **, $p < 0.01$. The values are expressed as percentages of basal and calculated as described under "Experimental Procedures." *B*, HepG2 and MCF-7 cells were transfected with either scrambled or Abl small interfering RNA (Sc-siRNA and Abl-siRNA, respectively) and serum-starved under "Experimental Procedures." Shown are blots with the indicated anti-phosphospecific antibody on crude lysates from either unstimulated cells (*lanes 1* and *4*) or from cells treated with 10 nM of either insulin (*lanes 2* and *5*) or IGF-I (*lanes 3* and *6*). Anti-Abl Western blot is also shown on the *bottom*. The means ± S.D. of densitometric analyses of three separate experiments are reported on the *right*. *, $p < 0.05$; **, $p < 0.01$. The values are expressed as percentages of basal and calculated as described under "Experimental Procedures." *C*, $abl^{-/-}arg^{-/-}$ and $abl^{\mathrm{WT}}arg^{-/-}$ mouse fibroblasts were serum-starved and incubated in the presence or absence of 1 μM STI571 as described under "Experimental Procedures." Shown are blots with the indicated anti-phosphotyrosine antibody on crude lysates from unstimulated cells (*lanes 1* and *4*) or from cells treated with 10 nM of either insulin (lanes 2 and 5) or IGF-I (*lanes 3* and *6*). Representative experiments are shown. The means ± S.D. of densitometric analyses of three separate experiments are reported on the *right*. *, $p < 0.05$; **, $p < 0.01$. The values are expressed as percentages of basal and calculated as described under "Experimental Procedures." *Untr.*, untreated.
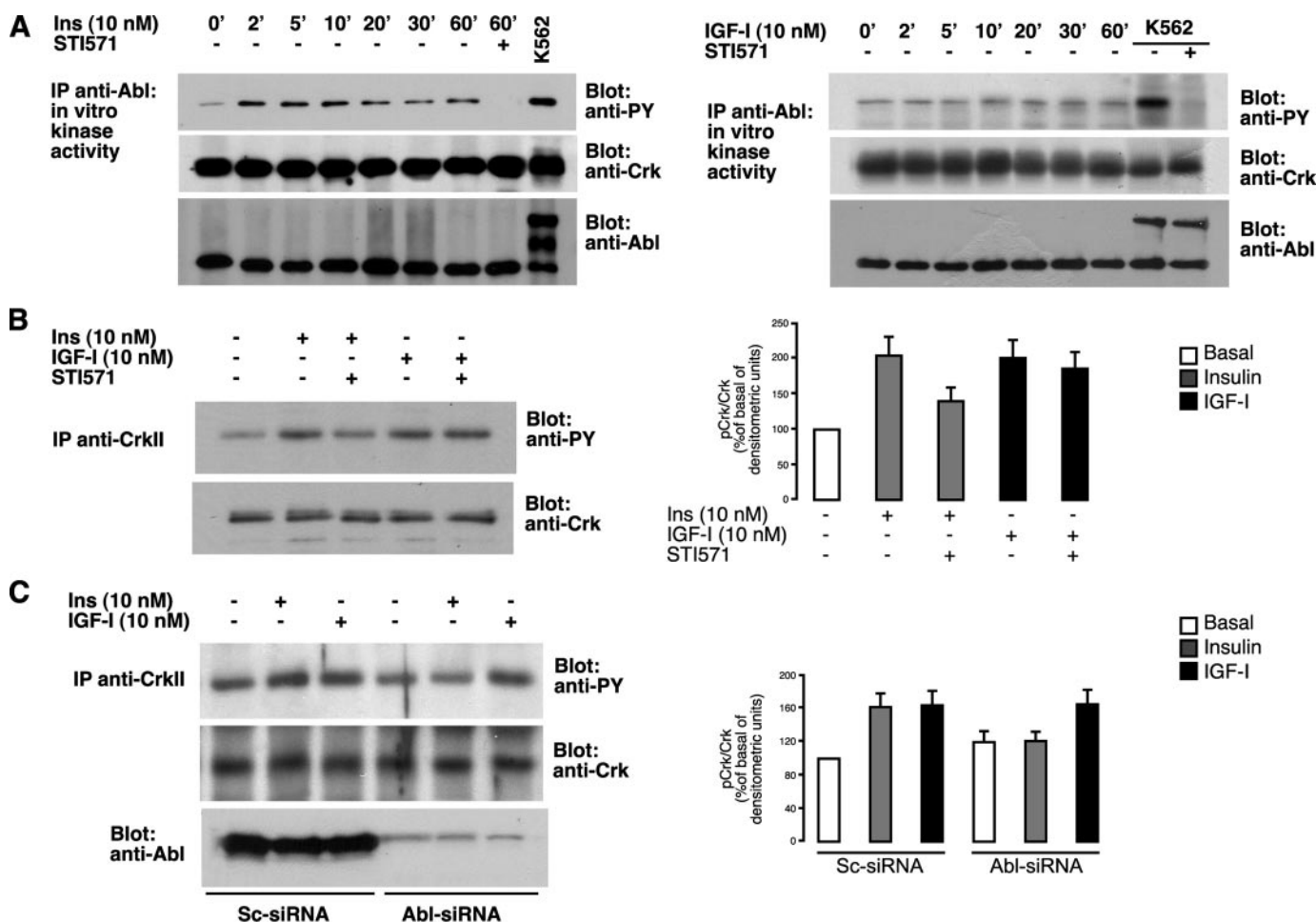
FIGURE 5. **Effect of insulin and IGF-I on c-Abl tyrosine kinase activity in HepG2 cells.** *A*, cells were serum-starved and incubated with either 10 nM insulin (on the *left*) or 10 nM IGF-I (on the *right*) for the indicated times, and c-Abl tyrosine kinase activity was evaluated using GST-Crk as a substrate in anti-Abl immunoprecipitates (*IP*). K562 cells, expressing the BCR-Abl oncoprotein, were used as a positive control. HepG2 cells were also incubated with the Abl inhibitor STI571 to demonstrate that Crk phosphorylation is Abl-specific. *Upper panel*, anti-Tyr(P) blot; middle panel: anti-Crk reblot; *lower panel*, anti-Abl reblot. The blots shown are representative of three separate experiments. *B*, cells were serum-starved and incubated in the presence or the absence of 1 μM STI571. The cells were then stimulated with 10 nM of either insulin or IGF-I for 10 min. Anti-Tyr(P) Western blot was performed on immunoprecipitated CrkII. Means ± S.D. of densitometric analyses of three separate experiments are reported on the *right*. The values are expressed as percentages of basal and calculated as described under "Experimental Procedures." *C*, HepG2 cells were transfected with either scrambled or Abl small interfering RNA (Sc-siRNA and Abl-siRNA, respectively) and serum-starved as indicated under "Experimental Procedures." The cells were then stimulated with 10 nM of either insulin or IGF-I for 10 min. Anti-Tyr(P) Western blot was performed on immunoprecipitated CrkII. Anti-Abl Western blot is also shown on the *bottom*. Representative experiments are shown. The means ± S.D. of densitometric analyses of three separate experiments are reported on the *right*. The values are expressed as percentages of basal and calculated as described under "Experimental Procedures."

ing the effect of insulin on FAK phosphorylation, HepG2 and MCF-7 cells were subjected to c-Abl silencing by siRNA (Fig. 6*B*). In accordance with data obtained with STI571, in cells treated with Abl-siRNA we observed FAK phosphorylation (instead of a dephosphorylation) in response to insulin (Fig. 6*B*, compare *lane 1* with *2* and *lane 4* with *lane 5*), whereas FAK response to IGF-I remained unchanged (Fig. 6*B*, compare *lane 1* with *lane 3* and *lane 4* with *lane 6*). Experiments performed in $abl^{-/-}arg^{-/-}$ and $abl^{WT}arg^{-/-}$ also confirmed these results (Fig. 6*C*, compare *lane 1* with *lane 2* and *lane 4* with *lane 5*). To confirm the effect of c-Abl activation on FAK phosphorylation, $abl^{-/-}arg^{-/-}$ cells were transfected with AblFKBP-WT constructs that encode for an Abl protein dimerized by the presence of the AP20187 compound (27). $Abl^{-/-}arg^{-/-}$ cells were also transfected with AblFKBP-KD (kinase defective) as a control. Anti-Tyr(P) Western blots revealed that AP20187 incubation resulted in AblFKBP-WT activation in transfected $abl^{-/-}$

$arg^{-/-}$ cells (Fig. 6*D*, *left panel*) and caused a dramatic FAK dephosphorylation in response to insulin stimulation (Fig. 6*D*, *right panel*). In contrast, AP20187 incubation did not change FAK phosphorylation in response to insulin in empty and in AblFKBP-KD-transfected cells.

Taken together our data suggest that insulin may induce FAK dephosphorylation via the activation of c-Abl tyrosine kinase. As a consequence, when c-Abl is inhibited, FAK phosphorylation (rather than a dephosphorylation) occurs in response to insulin, an effect similar to that observed with IGF-I stimulation.

FAK Mediates the Effect of c-Abl on Downstream IR Signaling Effectors—To confirm the role of FAK in the c-Abl tyrosine kinase signaling after insulin stimulation, we performed experiments in FAK$^{-/-}$ cells, fibroblasts derived from FAK knockout mice. As a control R6 cells, fibroblasts derived from littermates (11), were used.
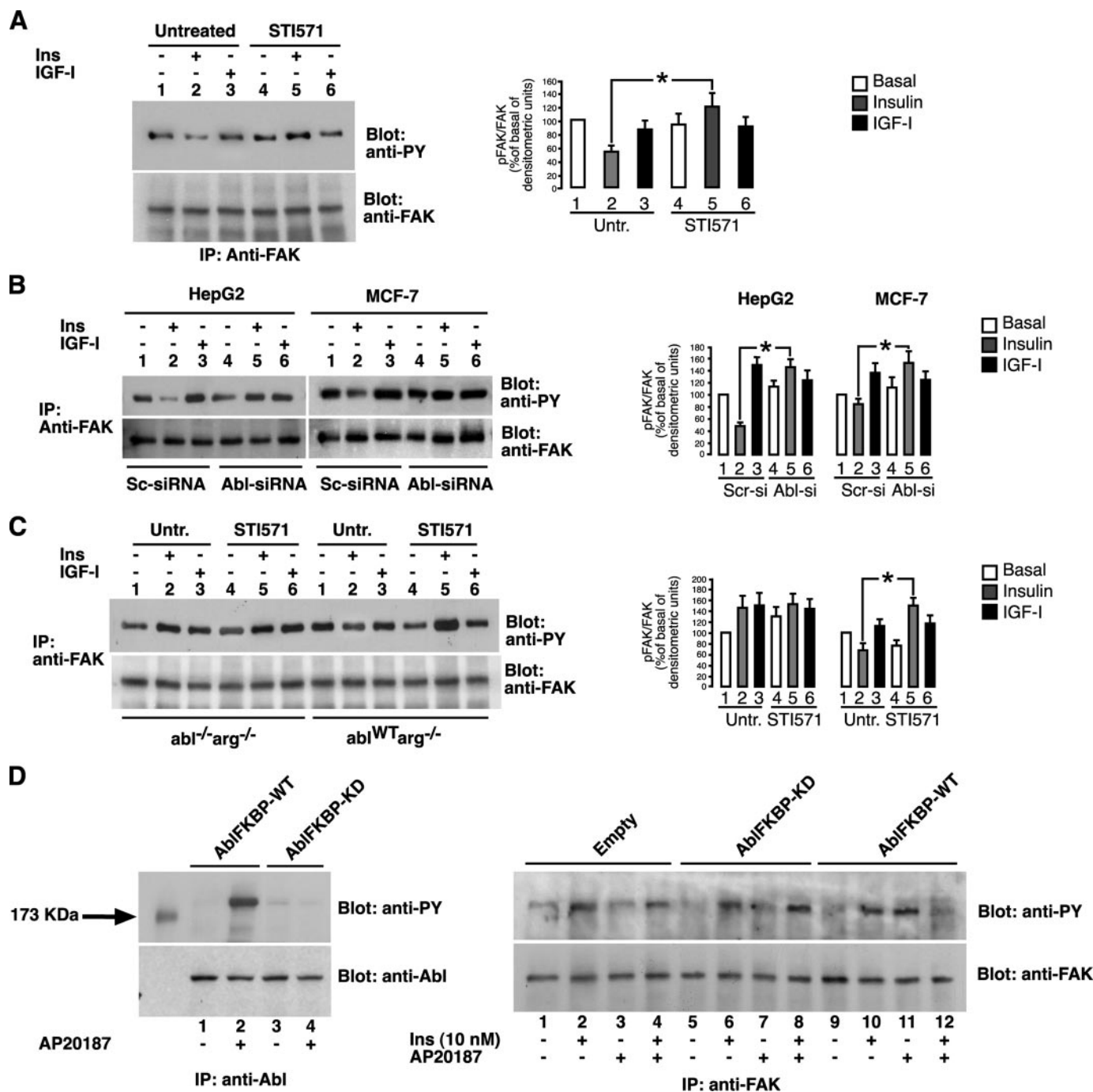
FIGURE 6. **Effect of c-Abl inhibition on FAK phosphorylation in response to either insulin or IGF-I.** *A*, HepG2 Cells were serum-starved, incubated in the presence or absence of 1 μM STI571, and stimulated with either insulin or IGF-I as described under "Experimental Procedures." Anti-phosphotyrosine Western blot of anti-FAK immunoprecipitates (*IP*) is shown. *Lanes 1* and *4*, unstimulated cells; *lanes 2* and *5*, cells treated with 10 nM insulin; *lanes 3* and *6*, cells treated with 10 nM IGF-I. Reprobing with anti-FAK antibody (*lower panel*) is also shown. Means $\pm$ S.D. of densitometric analyses of three separate experiments are reported on the *right*. *, $p < 0.05$; **, $p < 0.01$. The values are expressed as percentages of basal and calculated as described under "Experimental Procedures." *B*, HepG2 and MCF-7 cells were transfected with either scrambled or Abl small interfering RNA (Sc-siRNA and Abl-siRNA, respectively) and serum-starved as indicated under "Experimental Procedures." Anti-phosphotyrosine Western blot of anti-FAK immunoprecipitates is shown. *Lanes 1* and *4*, unstimulated cells; *lanes 2* and *5*, cells treated with 10 nM insulin; *lanes 3* and *6*, cells treated with 10 nM IGF-I. Reprobing with anti-FAK antibody (*lower panel*) is also shown. The means $\pm$ S.D. of densitometric analyses of three separate experiments are reported on the *right*. *, $p < 0.05$; **. $p < 0.01$. The values are expressed as percentages of basal and calculated as described under "Experimental Procedures." *C*, $abl^{-/-} arg^{-/-}$ and $abl^{WT} arg^{-/-}$ mouse fibroblasts were serum-starved and incubated in the presence or absence of 1 μM STI571 as described under "Experimental Procedures." Anti-phosphotyrosine Western blot of anti-FAK immunoprecipitates is shown. *Lanes 1* and *4*, unstimulated cells; *lanes 2* and *5*, cells treated with 10 nM insulin; *lanes 3* and *6*, cells treated with 10 nM IGF-I. Reprobing with anti-FAK antibody (*lower panel*) is also shown. Means $\pm$ S.D. of densitometric analyses of three separate experiments are reported on the *right*. *, $p < 0.05$; **, $p < 0.01$. The values are expressed as percentages of basal and calculated as described under "Experimental Procedures." *D*, $abl^{-/-} arg^{-/-}$ were transfected with either empty vector, AblFKBP-KD (kinase defective), or AblFKBP-WT, serum-starved, and incubated in the presence or the absence of AP20187 and insulin as indicated under "Experimental Procedures." *Left panel*, anti-phosphotyrosine Western blot of anti-Abl immunoprecipitates. *Right panel*, anti-phosphotyrosine Western blot of anti-FAK immunoprecipitates. *Lanes 1–4*, cells transfected with empty vector; *lanes 5–8*, cells transfected with AblFKBP-KD; *lanes 9–12*, cell transfected with AblFKBP-WT. Representative experiments are shown. *Untr.*, untreated.

Blots with a phosphospecific anti-ERK antibody revealed that in FAK$^{-/-}$ cells c-Abl inhibition by STI571 did not enhance ERK activation in response to increasing doses of insulin, whereas it did in R6 cells (Fig. 7*A*, compare *lanes 2* and *3* with *lanes 8* and *9*). Again, an increased ERK phosphorylation was observed in R6 cells exposed to STI571 only in response to

insulin, but not to IGF-I (Fig. 7*A*, compare *lanes 5* and *6 with lanes 11* and *12*).

We then tested the effect of STI571 c-Abl inhibition on insulin biological effects (Fig. 7*B*). Insulin effects were not affected in FAK$^{-/-}$ cells (Fig. 7*B*, compare *bar 2* with *bar 5*), whereas glycogen synthesis was inhibited, and cell proliferation and
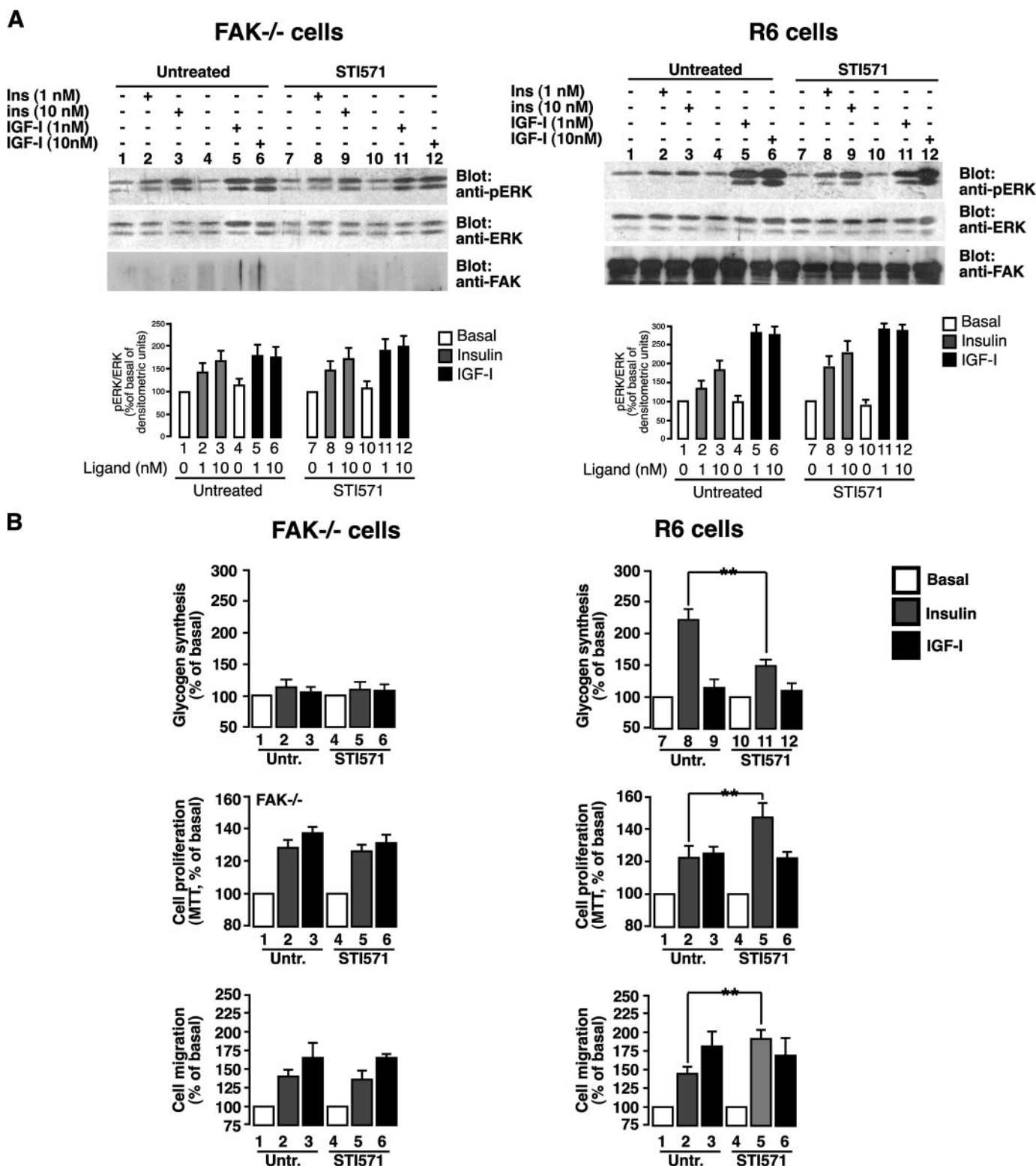
migration were enhanced in response to insulin in R6 cells (Fig. 7*B*, compare *bar 8* with *bar 11*). Also in this cell model, therefore, c-Abl inhibition provided results similar to those observed in HepG2, MCF-7, and $abl^{WT}arg^{-/-}$ cells. Finally, as in all other cell types, STI571 did not affect cell responses to IGF-I (Fig. 7*B*, compare *bar 3* with *bar 6* and *bar 9* with *bar 12*). Taken together, these results confirm in several cell models and by different experimental procedures that c-Abl is involved in IR signaling by affecting FAK phosphorylation in response to insulin stimulation.

DISCUSSION

Our results, obtained by independent experimental approaches including the evaluation of the insulin stimulation effect on c-Abl kinase activity, inhibition of c-Abl tyrosine kinase by STI571, and the use of c-Abl-null cells, indicate the involvement of c-Abl tyrosine kinase in IR signaling. At the same time, these data exclude the c-Abl involvement in IGF-IR signaling. The latter observation suggests that c-Abl may contribute to the difference in signaling and the biological effects of the two cognate receptors.

As far as c-Abl activation by insulin is concerned, c-Abl has already been reported to be involved in other tyrosine kinase receptor signaling, including PDGF-R, Met (hepatocyte growth factor receptor), and Trk (NGF receptor) (21, 22, 32, 33). Both activated PDGF-R and Met stimulate c-Abl tyrosine kinase activity (21, 22); whereas c-Abl activation by PDGF results in increased cell proliferation (21), c-Abl activation by Met exerts a negative regulatory effect and is concomitant with reduced cell migration in response to hepatocyte growth factor in thyroid cancer cells (22). c-Abl activation by Trk results in CrkII phosphorylation, axonal outgrowth, and guidance (34). These observations highlight the role of c-Abl tyrosine kinase in growth factor receptor signaling, although the biological role and consequences of c-Abl activation may be different (opposite) depending on the receptor involved, the signaling pathway, and the cell context. Here we describe the role of c-Abl in insulin receptor signaling and metabolic effects; by inhibiting insulin-induced ERK activation and enhancing, at the same time, Akt activation, c-Abl confers specificity to the IR signaling, leading to predominant metabolic effects. It is noteworthy that c-Abl does not influence the predominant mitogenic

effects of the cognate IGF-IR. The exact pathway leading to the activation of c-Abl tyrosine kinase after IR stimulation by insulin, however, remains to be elucidated.

Here we report that cell exposure to insulin stimulates c-Abl tyrosine kinase activity and that, in turn, this causes FAK dephosphorylation, and as a consequence, it leads to a predominant phosphorylation of the Akt/GSK-3β and to glycogen synthesis. In contrast, when c-Abl is inhibited or absent, FAK is phosphorylated after insulin stimulation, and this results in an increased effect of insulin on the ERK pathway activation, cell proliferation, and migration. We also provide evidence that the effect of c-Abl is not dependent on proximal events of IR signaling, including receptor β-subunit and/IRS-1 phosphorylation and the recruitment of the small adapter protein p85 and Grb2 but rather on the distal effect on FAK phosphorylation. When c-Abl is inhibited or absent, a dramatic change in the response of FAK to insulin stimulation occurs, and insulin stimulates FAK phosphorylation in a manner similar to that of IGF-I. c-Abl inhibition, therefore, selectively modifies IR signaling and effects in such a way that IR signaling will mimic IGF-IR signaling in respect to FAK phosphorylation. c-Abl-dependent changes of FAK phosphorylation are a necessary step for the effect of c-Abl on insulin signaling; in cells devoid of FAK (FAK$^{-/-}$ cells) c-Abl inhibition is without effect on insulin signaling and actions. These results are in accordance also with previous observations that a functional FAK is required for the metabolic effects of insulin in HepG2 cells (35) and L6 myotubes (19).

The specific role of FAK phosphorylation or dephosphorylation, however, requires further investigations. It has been shown that insulin is not able to stimulate FAK dephosphorylation in cells transfected with an IR mutant, where Tyr^{1210} is replaced by Phe (36). Interestingly, in these cells, insulin is more effective in stimulating ERK rather than phosphatidylinositol 3-kinase when compared with cells transfected with the wild type IR (36). These results further remark the importance of FAK dephosphorylation in restraining the mitogenic effect and enhancing the metabolic effects of insulin.

Because c-Abl is activated by cell adhesion (20), it is reasonable to suppose that it may play a relevant role in the complex interplay between integrin and insulin signaling, where inte-

---

FIGURE 7. **Role of FAK in mediating the effect of c-Abl on insulin actions: experiments in FAK$^{-/-}$ and R6 cells.** *A*, effect of c-Abl inhibition on insulin stimulated FAK phosphorylation in FAK$^{-/-}$ (*top panels*) and R6 (*bottom panels*) mouse fibroblasts. The cells were serum-starved and incubated in the presence or absence of 1 μM STI571 as described under "Experimental Procedures." Western blots of crude lysates from unstimulated cells (*lanes 1, 4, 7,* and *10*) or cells treated either with insulin at 1 nM (*lanes 2* and *8*) and 10 nM (*lanes 3* and *9*) or with IGF-I at 1 nM (*lanes 5* and *11*) and 10 nM (*lanes 6* and *12*). *Top panels*, blots with anti-phospho-ERK antibody; *middle panels*, anti-ERK antibody; *bottom panels*, anti-FAK antibody. The blots shown are representative of three separate experiments. The means ± S.D. of densitometric analyses of three separate experiments are reported on the *bottom*. The values are expressed as percentages of basal and calculated as described under "Experimental Procedures." *B*, effect of c-Abl inhibition on insulin effects in FAK$^{-/-}$ (*left graphs*) and R6 (*right graphs*) mouse fibroblasts. The *top panels* show glycogen synthesis. The cells were serum-starved and incubated in the absence (*bars 1–3* and *7–9*) or the presence (*bars 4–6* and *10–12*) of 1 μM STI571 in low glucose medium as described under "Experimental Procedures." Glycogen synthesis in the absence (*white bars*) or the presence of 10 nM of either insulin (*gray bars*) or IGF-I (*black bars*) was evaluated as [^{14}C]glucose incorporation into glycogen. The numbers are expressed as percentages of basal and indicate the means ± S.D. of three separate experiments performed in triplicate. **, $p < 0.01$. The *middle panels* show cell proliferation. The cells were plated onto 96-multiwell and grown for 5 days in the absence (*bars 1–3* and *7–9*) or the presence (*bars 4–6* and *10–12*) of 1 μM STI571 and the indicated growth factors. *White bars*, unstimulated cells; *gray bars*, cells stimulated with 10 nM insulin; *black bars*, cells stimulated with 10 nM IGF-I. After incubation with MTT, the plates were read at 590 nm as described under "Experimental Procedures." The numbers are expressed as percentages of basal and indicate the means ± S.D. of three experiments performed in triplicate. **, $p < 0.01$. The *bottom panels* show cell migration. The cells were first incubated in the absence (*bars 1–3* and *7–9*) or the presence (*bars 4–6* and *10–12*) of 1 μM STI571 as described under "Experimental Procedures." The cells were then collected and allowed to migrate in lower side collagen-coated transwells for 6 h in the absence (*white bars*) or the presence of 10 nM of either insulin (*gray bars*) or IGF-I (*black bars*) in the presence (*bars 4–6* and *10–12*) or absence (*bars 1–3* and *7–9*) of 1 μM STI571. The numbers are expressed as percentages of basal and are the means ± S.D. of three separate experiments performed in triplicate. **, $p < 0.01$. *Untr.*, untreated.

grins determine the cell relationship with the extracellular matrix and insulin regulates the cell energy metabolism and storage. Indeed, it has been reported that cell detachment from the extracellular matrix results in a dramatic switch of the FAK phosphorylation in response to insulin, similar to that observed when c-Abl is inhibited (13). When cells attach, c-Abl tyrosine kinase is activated, and this may cause FAK dephosphorylation in response to insulin, and consequently, inhibition of the cell ability to respond to insulin stimulation in terms of further migration and proliferation, whereas the cell metabolic activity is potentiated. In contrast, when c-Abl activity is down-regulated, as it occurs when cells detach, metabolic effects of insulin (like glycogen synthesis) are blunted, whereas effects on cell proliferation and migration are potentiated to an extent similar to that elicited by IGF-I. By this mechanism detached cells may obtain the biochemical instruments favoring their relocalization and proliferation. These data may also explain why insulin can cause FAK phosphorylation or dephosphorylation depending on different cell context and experimental conditions (13, 15–19).

We have not investigated the mechanism underlying c-Abl tyrosine kinase effect on FAK response to insulin stimulation. Some indirect evidence supports a role for CrkII as a possible link between c-Abl and FAK phosphorylation; carboxyl deletion mutants of CrKII enhance FAK phosphorylation (37), reproducing the condition when c-Abl activity is suppressed.

In conclusion the present results suggest that c-Abl is an important component of the intracellular signaling pathway activated by insulin, able to confer specificity to IR signaling by determining FAK phosphorylation or dephosphorylation. When c-Abl is inhibited or absent, insulin stimulation causes FAK phosphorylation, thereby mimicking IGF-I stimulation. Under this condition the metabolic effects of insulin are attenuated, while cell proliferation and migration are enhanced. c-Abl deregulation, therefore, could be involved in a variety of pathological conditions including insulin resistance, abnormal proliferative effects, and cancer, a condition in which this mechanism may provide a selective advantage to malignant cells in terms of both proliferation and invasiveness. c-Abl may be regarded, therefore, as a molecular switch or rheostat that determines the quality of cell response to insulin by restraining insulin signaling output to metabolic effects. Further studies of this mechanism may result from interest in different pathological conditions, and c-Abl targeting by specific molecules may prove useful for designing new therapeutic strategies aimed at controlling cell responsiveness to insulin.

REFERENCES

1. Kido, Y., Nakae, J., and Accili, D. (2001) *J. Clin. Endocrinol. Metab.* **86,** 972–979
2. Valentinis, B., and Baserga, R. (2001) *Mol. Pathol.* **54,** 133–137
3. Nakae, J., Kido, Y., and Accili, D. (2001) *Endocr. Rev.* **22,** 818–835
4. Mitra, S. K., Hanson, D. A., and Schlaepfer, D. D. (2005) *Nat. Rev. Mol. Cell. Biol.* **6,** 56–68
5. Leventhal, P. S., Shelden, E. A., Kim, B., and Feldman, E. L. (1997) *J. Biol. Chem.* **272,** 5214–5218
6. Schlaepfer, D. D., Hanks, S. K., Hunter, T., and van der Geer, P. (1994) *Nature* **372,** 786–791
7. Harte, M. T., Hildebrand, J. D., Burnham, M. R., Bouton, A. H., and Parsons, J. T. (1996) *J. Biol. Chem.* **271,** 13649–13655
8. Hildebrand, J. D., Schaller, M. D., and Parsons, J. T. (1995) *Mol. Biol. Cell* **6,** 637–647
9. Ruest, P. J., Shin, N. Y., Polte, T. R., Zhang, X., and Hanks, S. K. (2001) *Mol. Cell. Biol.* **21,** 7641–7652
10. Tachibana, K., Urano, T., Fujita, H., Ohashi, Y., Kamiguchi, K., Iwata, S., Hirai, H., and Morimoto, C. (1997) *J. Biol. Chem.* **272,** 29083–29090
11. Sieg, D. J., Hauck, C. R., Ilic, D., Klingbeil, C. K., Schaefer, E., Damsky, C. H., and Schlaepfer, D. D. (2000) *Nat. Cell Biol.* **2,** 249–256
12. Renshaw, M. W., Price, L. S., and Schwartz, M. A. (1999) *J. Cell Biol.* **147,** 611–618
13. Baron, V., Calleja, V., Ferrari, P., Alengrin, F., and Van Obberghen, E. (1998) *J. Biol. Chem.* **273,** 7162–7168
14. Pillay, T. S., Sasaoka, T., and Olefsky, J. M. (1995) *J. Biol. Chem.* **270,** 991–994
15. Cheung, A. T., Wang, J., Ree, D., Kolls, J. K., and Bryer-Ash, M. (2000) *Diabetes* **49,** 810–819
16. Knight, J. B., Yamauchi, K., and Pessin, J. E. (1995) *J. Biol. Chem.* **270,** 10199–10203
17. Schaller, M. D., Borgman, C. A., Cobb, B. S., Vines, R. R., Reynolds, A. B., and Parsons, J. T. (1992) *Proc. Natl. Acad. Sci. U. S. A.* **89,** 5192–5196
18. Wang, Q., Bilan, P. J., and Klip, A. (1998) *Mol. Biol. Cell* **9,** 3057–3069
19. Huang, D., Khoe, M., Ilic, D., and Bryer-Ash, M. (2006) *Endocrinology* **147,** 3333–3343
20. Taagepera, S., McDonald, D., Loeb, J. E., Whitaker, L. L., McElroy, A. K., Wang, J. Y., and Hope, T. J. (1998) *Proc. Natl. Acad. Sci. U. S. A.* **95,** 7457–7462
21. Plattner, R., Kadlec, L., DeMali, K. A., Kazlauskas, A., and Pendergast, A. M. (1999) *Genes Dev.* **13,** 2400–2411
22. Frasca, F., Vigneri, P., Vella, V., Vigneri, R., and Wang, J. Y. (2001) *Oncogene* **20,** 3845–3856
23. Ren, R., Ye, Z. S., and Baltimore, D. (1994) *Genes Dev.* **8,** 783–795
24. Rosen, M. K., Yamazaki, T., Gish, G. D., Kay, C. M., Pawson, T., and Kay, L. E. (1995) *Nature* **374,** 477–479
25. Lin, W. H., Huang, C. J., Liu, M. W., Chang, H. M., Chen, Y. J., Tai, T. Y., and Chuang, L. M. (2001) *Genomics* **74,** 12–20
26. Kapeller, R., Moriarty, A., Strauss, A., Stubdal, H., Theriault, K., Siebert, E., Chickering, T., Morgenstern, J. P., Tartaglia, L. A., and Lillie, J. (1999) *J. Biol. Chem.* **274,** 24980–24986
27. Smith, K. M., and Van Etten, R. A. (2001) *J. Biol. Chem.* **276,** 24372–24379
28. Koleske, A. J., Gifford, A. M., Scott, M. L., Nee, M., Bronson, R. T., Miczek, K. A., and Baltimore, D. (1998) *Neuron* **21,** 1259–1272
29. Pandini, G., Frasca, F., Mineo, R., Sciacca, L., Vigneri, R., and Belfiore, A. (2002) *J. Biol. Chem.* **277,** 39684–39695
30. Koval, A. P., Blakesley, V. A., Roberts, C. T., Jr., Zick, Y., and Leroith, D. (1998) *Biochem. J.* **330,** 923–932
31. Beitner-Johnson, D., and LeRoith, D. (1995) *J. Biol. Chem.* **270,** 5187–5190
32. Escalante, M., Courtney, J., Chin, W. G., Teng, K. K., Kim, J. I., Fajardo, J. E., Mayer, B. J., Hempstead, B. L., and Birge, R. B. (2000) *J. Biol. Chem.* **275,** 24787–24797
33. Yano, H., Cong, F., Birge, R. B., Goff, S. P., and Chao, M. V. (2000) *J. Neurosci. Res.* **59,** 356–364
34. Lu, Q., Mukhopadhyay, N. K., Griffin, J. D., Paredes, M., Medina, M., and Kosik, K. S. (2002) *J. Neurosci. Res.* **67,** 618–624
35. Huang, D., Cheung, A. T., Parsons, J. T., and Bryer-Ash, M. (2002) *J. Biol. Chem.* **277,** 18151–18160
36. Van der Zon, G. C., Ouwens, D. M., Dorrestijn, J., and Maassen, J. A. (1996) *Biochemistry* **35,** 10377–10382
37. Zvara, A., Fajardo, J. E., Escalante, M., Cotton, G., Muir, T., Kirsch, K. H., and Birge, R. B. (2001) *Oncogene* **20,** 951–961
38. Sieg, D. J., Hauck, C. R., Ilic, D., Klingbeil, C. K., Schaefer, E., Damsky, C. H., and Schlaepfer, D. D. (2000) *Nat. Cell Biol.* **2,** 249–256